Available online at www.sciencedirect.com
ScienceDirect
Polymer 47 (2006) 8116–8122
polymer
www.elsevier.com/locate/polymer

Surface-active fluorocarbon end-functionalized polylactides

Lian R. Hutchings, Amilcar Pillay Narrainen, Stuart M. Eggleston, Nigel Clarke, Richard L. Thompson*

Department of Chemistry, Durham University, Science Site, South Road, Durham, DH1 3LE, UK

Received 20 July 2006; received in revised form 21 September 2006; accepted 25 September 2006
Available online 16 October 2006

Abstract

The synthesis and surface properties of a $2 \times C_8F_{17}$ fluorocarbon di-functionalized poly(D,L-lactide), "F2PLA" are described. Small fractions ~5% w/w of F2PLA, when blended with unfunctionalized poly(D,L-lactide), "PLA", render the surface both hydrophobic and lipophobic. Contact angle analysis indicates that the properties of the blend surface approach those of PTFE. Rutherford backscattering analysis of the surface shows that at saturation, approximately 50% of the blend surface is covered by C_8F_{17} fluorocarbon units. Using self-consistent field theory simulations, we estimate that adsorption of the F2PLA is characterized by a thermodynamic sticking energy of the difunctional group of approximately 6 k_BT. Bilayer samples were prepared in which a blend of F2PLA in PLA was initially covered with a layer of pure PLA. The rate of surface modification in these films was analysed to obtain a diffusion coefficient of up to 160 $nm^2\ s^{-1}$ for 21.6 kg/mol F2PLA at 90 °C.

Keywords: Adsorption; Surface modification; Functionalized polymers

1. Introduction

Many applications of polymers require combinations of properties that place specific demands on the bulk and surface of material. Physical properties such as stiffness, toughness, viscosity and optical clarity are associated with the bulk, whilst adhesion, water or oil repellency, biocompatibility and tribology are regarded as surface properties. Surface properties are dependent upon only the first few nanometers of a material; only a miniscule fraction of the total volume of macroscopic objects. For low volume, high value applications, it may be acceptable to ignore this inefficiency and use the same material throughout an object. Increasingly, both the financial and environmental cost of such an approach will become prohibitive. Moreover, it is highly unlikely that the optimum combination of bulk and surface properties will be found in any single component system.

Various strategies have been employed to improve the properties of commodity polymers. Surfaces may be modified using an additional processing step such as corona treatment or reactive functionalisation [1,2]. Additionally, a wide variety of coating methods, such as co-extrusion of a second layer onto the bulk polymer or roll-coating have also been developed [3]. Both of these approaches are used in commercial applications, but it is recognized that in addition to the inconvenience of the second processing step, there are also technological challenges ensuring that the coated surface has the required level of durability.

An appealing alternative is the use of additives to the polymer which achieve the necessary modification during processing. These additives may be small molecules such as plasticisers, solid particles in the case of composites, or they may be other polymers. The adsorption and surface structure of end-functionalized polymers have been studied in detail for the last two decades [4–15]. As well as being of academic interest, they are inherently compatible with unfunctionalized polymers of the same repeat unit structure. The functional groups can be a very small proportion of the size of the end-functional polymer; therefore the adsorption of whole polymer chains induced by a single functional group should be regarded as an extremely efficient process. The disadvantage

* Corresponding author. Tel.: +44 191 334 2139; fax: +44 191 384 4737.
E-mail address: r.l.thompson@dur.ac.uk (R.L. Thompson).

0032-3861/$ - see front matter © 2006 Elsevier Ltd. All rights reserved.
doi:10.1016/j.polymer.2006.09.050

of having such a small functional group is that even though it may promote the adsorption of a polymer chain, changes to the surface properties as a result of the adsorption process are very small. For end-functionalized polymers to have useful surface modification properties in blends, it is necessary to increase size of the functional unit relative to the polymer chain. Recently it has been shown that it is possible to overcome this limitation by incorporating multiple functional groups to a polymer chain end via a dendritic functional group [15,16]. The synthesis of dendrons is somewhat arduous so it is expedient to minimise the generation number of the dendron by maximising the size of the functional group that is appended. Although diblock copolymer architectures could satisfy the requirement for a large functional group, the dendritic approach offers absolute control over the precise size of the functionality. This is an important factor as it may help to avoid the problems of microphase separation and micellisation that limit the usefulness of block copolymers in polymer blends [17,18]. Whilst there is no guarantee that a different macromolecular structure will inhibit micellisation, we note that the sequence of mesophase behaviour reported for dendritically functionalized polymers appears to differ significantly from that of the diblock copolymers [19,20]. Having a linear polymer chain chemically bonded to the functional group raises the intriguing possibility of surface modification with an additive that is essentially anchored to the bulk material.

In this paper we describe how this approach may be applied to poly(D,L-lactide). Polylactides are moderately hydrophilic, and it is of interest to control the hydrophilicity since this may in turn provide a simple means of controlling the rate of biodegradation. Osawa et al. [21] have recently shown that by transcribing the pattern from a hydrophobic leaf it is possible to render a poly-caprolactone surface super-hydrophobic. This approach was successful because the leaf surface that was used to template the polymer surface had an extremely large surface area. However, applying this methodology to large areas of polymers of arbitrary shape is not trivial, and there is still a need for a general approach towards hydrophobic biodegradable polymers. Here we show that di-functionalized polymer chains may be used to promote surface adsorption with far greater efficiency than that has previously been seen for mono-end-functionalized polymers in blends [10,13,22]. The adsorption of difunctional polylactide is explored as a function of blend concentration and the accompanying modification to the surface properties is also discussed.

2. Experimental section

2.1. Materials

Poly(D,L-lactide), 'PLA' ($M_w = 96.1$ kg/mol, M_w/M_n of 2.11)[1] was purchased from Aldrich, U.K. and used as received. Di-fluorocarbon functionalized initiator was prepared by first brominating 3-(perfluorooctyl)propanol using CBr_4 and PPh_3. The product was coupled with 3,5-dihydroxybenzyl alcohol in the presence of K_2CO_3 and 18-crown-6 to give the initiator, 3,5(di-3-(perfluorooctyl)propyloxy)benzyl alcohol. Di-fluorocarbon end-functionalized poly(D,L-lactide), "F2PLA", (M_w of 21.6 kg/mol, M_w/M_n of 1.76) was prepared by ring opening polymerisation as follows. Tin(II) octoate (Aldrich) was dissolved in benzene and the stock solution was degassed and kept under a nitrogen atmosphere. Di-fluorocarbon functionalized benzyl alcohol initiator (0.113 g, 0.107 mmol), tin(II) octoate catalyst (0.037 mmol) and D,L-lactide monomer (1.08 g, 7.49 mmol) were added to an evacuated Schlenk tube in a glove box. The tube was filled with nitrogen, fitted with a rubber septum and lowered in a thermostatically controlled oil-bath at 155 °C. The reaction was left for 5 h under nitrogen. NMR analysis was used to monitor the disappearance of the CH_2OH peak of the benzyl alcohol, thus confirming the absence of unreacted initiator. The magnitude of the NMR signal from the terminal $CH(CH_3)OH$ groups when compared to the initiator confirmed that at least 80% of the PLA chains were coupled to the di-fluorocarbon functionalized initiator. Purification was achieved by allowing the mixture to cool, diluting in THF and precipitating in hexane four times. The polymer was dried under vacuum for 2 days. The chemical structures of the initiator and polymer are shown in Fig. 1.

2.2. Film preparation

F2PLA and PLA homopolymer were co-dissolved in THF in the desired proportions, and then spin-cast onto silicon wafers. In order to remove all traces of solvent, and to allow the polymers to relax to their equilibrium configuration, the coated wafers were annealed at 90 °C for 1 h under vacuum. Bilayer films were prepared in order to study the diffusion of F2PLA in PLA. In this case a 510 nm thick 20% blend of F2PLA in PLA was spin-cast onto a silicon wafer and annealed at 90 °C for 1 h. A second film of pure PLA, 445 nm total thickness, was spin-cast onto a large glass microscope slide and then transferred onto the coated silicon substrate by floatation on high purity water. Film thicknesses were characterized via optical reflectometry and found to be

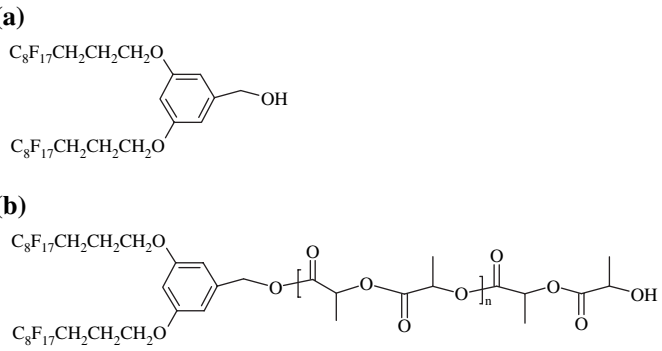

Fig. 1. Structures for (a) fluorocarbon functionalized benzyl alcohol initiator and (b) F2PLA polymer.

[1] Molecular weight data were obtained relative to polystyrene standards via size exclusion chromatography with THF as the eluent.

consistent within ±10% of the measured value. The bilayer films were thoroughly dried at room temperature and then annealed for periods of up to 2 h under vacuum at 90 °C. Since all of the samples were annealed in the absence of oxygen and water, degradation is not expected to be significant in these experiments.

2.3. Contact angle analysis

The hydrophobicity and lipophobicity of polylactide blend surfaces were measured by contact angle analysis. The average of at least three separate advancing contact angle measurements was determined yielding contact angles with a precision of ±2°. Measurements were carried out with water and dodecane and polar and non-polar contact fluids, respectively, from which the polar and dispersive components of the surface energy may be estimated.

2.4. Ion beam analysis

Rutherford backscattering (RBS) measurements enabled the determination of the near-surface distribution of fluorocarbon for each film. This technique is discussed in greater detail elsewhere [23,24]. A 1800 keV $^4He^+$ beam was brought onto the sample surface at 85° to the sample normal (i.e. 5° grazing incidence). Backscattered $^4He^+$ ions were detected with 19 keV resolution using a PIPS detector at 170° to the incident beam. Since fluorine is the most massive element present at the polymer surface, $^4He^+$ recoils are detected at higher energy than recoils from the other elements, C and O within the sample.

Due to the fact that both polylactide and fluorocarbons are somewhat susceptible to beam damage, a diffuse ion beam of 2 mm diameter was used. At 5° grazing incidence the footprint of the beam was an ellipse of approximately 23 mm × 2 mm. The beam charge on each spot was restricted to 0.5 μC, and samples were cooled to below −50 °C to minimise degradation. With these precautions, consecutive measurements on the same spot yielded indistinguishable spectra; therefore we are confident that our results contain no artefacts due to beam damage. By summing data from at least 12 measurements on separate spots, sufficiently good statistical quality was obtained to analyse the near-surface fluorocarbon distribution.

3. Results

Results for contact angle measurements are shown in Fig. 2. The contact angles of both dodecane and water rise sharply with increasing F2PLA content in each film towards a plateau at approximately 5% w/w additive. The increase in water contact angle from 75° in the case of pure PLA homopolymer towards 105° clearly demonstrates that even at rather low additive concentrations, there is a marked increase in the hydrophobicity of the blended film surface. The contact angle of pure PTFE is of the order of 108° for smooth surfaces, and more if the surface has been treated to increase its roughness [2]. It therefore appears that these additives are able to confer sufficient fluorocarbon to the PLA surface such that it approaches the hydrophobicity of PTFE. It is worth noting at this point that the concentration axis in Fig. 2 refers to the concentration of F2PLA, and not the concentration of fluorocarbon functional groups. The fluorocarbon concentration is much lower since the two C_8F_{17} groups per F2PLA chain account for only 834 g/mol of the polymer chain, which has a molecular weight of 21.6 kg/mol. The saturation concentration of 5% F2PLA corresponds to approximately 0.2% fluorocarbon content in the polymer blend. Dodecane was found to spread on pure PLA films; therefore the contact angle could not be measured. However, even at 1% F2PLA additive concentration the measurable contact angle indicates an appreciable level of lipophobicity due to the surface concentration of fluorocarbon. With increasing F2PLA content, the contact angle of dodecane on the blend surfaces follows a qualitatively similar trend to that observed for water.

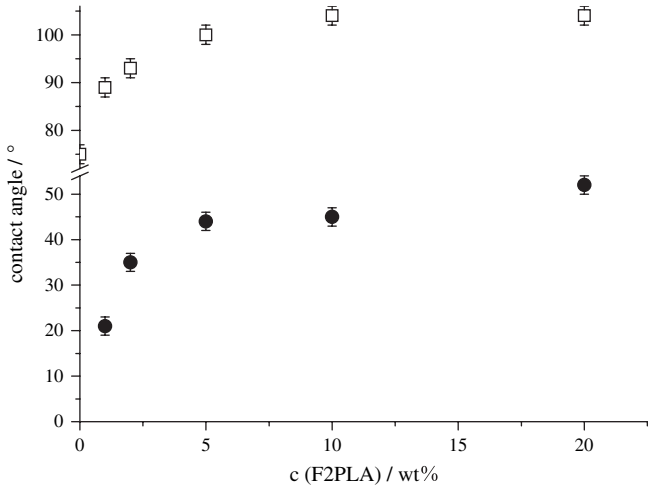

Fig. 2. Contact angle data for water and dodecane on the surface of F2PLA/PLA blends.

RBS data for each film containing F2PLA are shown in Fig. 3. The elemental markers indicate the maximum possible recoil energy of $^4He^+$ ions from each element on the surface. If silicon due to the substrate were present close to the film surface, then $^4He^+$ recoils from Si could be detected at energies of up to 1025 keV. However, the combination of film thickness and sample orientation with respect to the beam and detector greatly reduces the energy of recoils from Si, and these were always at energies of 600 keV or less. The films containing 1%, 2%, and 5% PLA show sharp 'steps' in the detected counts at C and O, which are expected for a thick film of polylactide. These steps are less clearly visible in the two highest concentrations simply because these films were slightly thinner, and $^4He^+$ recoils from the silicon substrate are detected in the low energy end of the RBS spectrum. The small peak at approximately 770 keV arises from fluorine at the sample surface, which is present at a greater concentration than in the bulk of the film. The fluorocarbon peak is well separated from the step in the profile due to oxygen, and (when present) the background from Si, allowing accurate analysis of

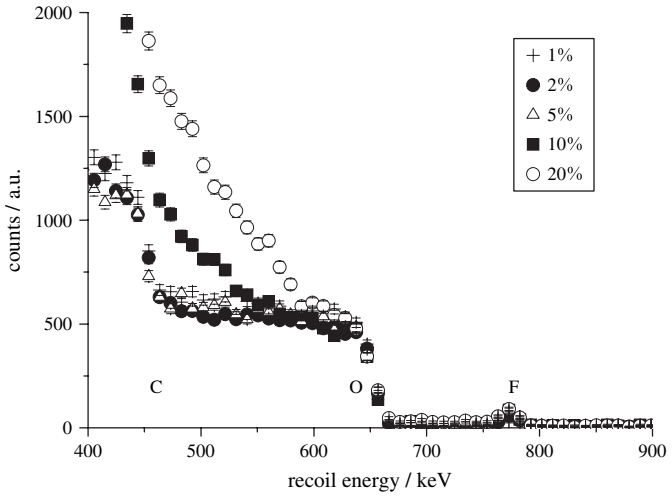

Fig. 3. Rutherford backscattering data for F2PLA/PLA blends. The elemental markers indicate the maximum recoil energy of $^4He^+$ from each element in the film surface.

the near-surface fluorocarbon concentration. Data for model simulations, in which the RBS spectrum due to a thin layer of C_8F_{17} on a thick film of PLA, are shown in Fig. 4. Simulations were carried out using the SIMNRA program [25] and Rutherford scattering cross sections [24]. The thickness of the C_8F_{17} layer was allowed to vary to provide the best fit to the experimental data, and the surface concentration of fluorocarbon from this layer was determined. A very small background contribution was detected at recoil energies greater than 800 keV due to traces of Sn used in the F2PLA synthesis. The concentration of Sn was assumed to be constant throughout the bulk of the film, and was included in the model used to fit the data. When this correction was made, and the appropriate amount of fluorine due to the bulk concentration of F2PLA was also included, excellent agreement between simulation and data in the energy range 675–750 keV was observed.

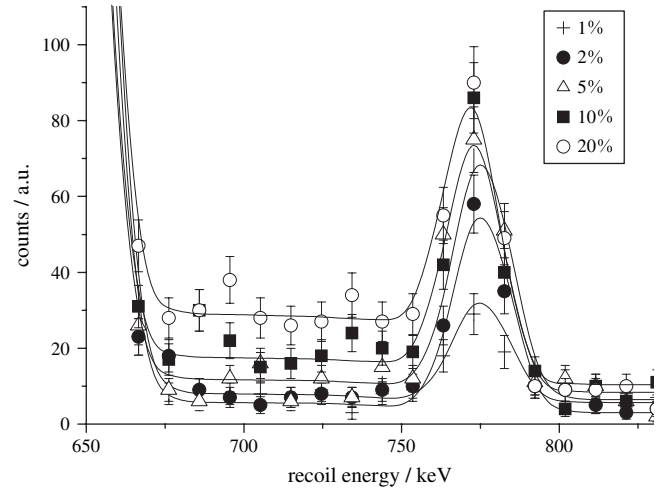

Fig. 4. Experimental data and fits (solid curves) to fluorine peak in RBS spectra used to characterise F2PLA surface adsorption.

4. Discussion

The contact angle results show that with increasing F2PLA concentration, there is a clear increase in both hydrophobicity and lipophobicity of the blend surface. Both observations are consistent with the F2PLA adsorbing at the surface of the annealed blend, and replacing polylactide with fluorocarbon. Whilst the adsorption of end-functionalized polymers to surfaces is well documented, changes in contact angle with mono-functionalized polymers have been negligible [26] or modest (<5°) [15,22], and have been restricted to end-functionalized polymers that are well below their entanglement molecular weight. Here the inclusion of two relatively large fluorocarbon groups has caused an increase in water contact angle of approximately 30°, and molecular weight of the end-functionalized polylactide chain is approximately five times the entanglement molecular weight, M_e (=3959 g/mol) [27]. Furthermore, we are unaware of any previous report showing an increase in lipophobicity as a result of end-functionalized polymer adsorption.

It is of interest to quantify the change in surface energy of the blend as a result of F2PLA adsorption. By using at least two contact fluids, it is possible to separate the polar and dispersive contributions to the surface energy [28,29]. The contact angle, θ is a function of the liquid surface energy, γ_l, the dispersive components of the solid and liquid surface energies, γ_s^d and γ_l^d and the polar components of the solid and liquid surface energies, γ_s^p and γ_l^p,

$$\cos\theta = \frac{2\sqrt{\gamma_s^d\gamma_l^d}}{\gamma_l} + \frac{2\sqrt{\gamma_s^p\gamma_l^p}}{\gamma_l} - 1 \qquad (1)$$

In our analysis, we used deionized water ($\gamma_l = 72.8\ \mathrm{mJ\,m^{-2}}$, $\gamma_l^d = 21.8\ \mathrm{mJ\,m^{-2}}$, $\gamma_l^p = 51.0\ \mathrm{mJ\,m^{-2}}$) [28] and dodecane ($\gamma_l = 25.4\ \mathrm{mJ\,m^{-2}}$, $\gamma_l^d = 25.4\ \mathrm{mJ\,m^{-2}}$, $\gamma_l^p = 0$) [30]. The contact angle with each fluid provides two equations from which the two unknowns γ_s^p and γ_s^d may be resolved. The large difference in polarity between water and dodecane helps to ensure that the solution to the equations is not ill-conditioned. Results derived for the polar and dispersive components of the solid surface energy are shown in Fig. 5. The error bars shown at the maximum and minimum F2PLA concentrations show the uncertainty in these values arising from the uncertainty in each contact angle measurement. Adsorption of F2PLA at the blend surface reduces the overall surface energy by reducing both the polar and dispersive components of the surface energy.

If one assumes that the surface energy is related to the surface energy of the pure components by their relative surface coverage, then it follows that the cosine of the contact angle, $\cos\theta$, has the same form [22]

$$\cos\theta = \phi_{FC}\cos\theta_{FC} + (1-\phi_{FC})\cos\theta_{PLA} \qquad (2)$$

where θ_{FC} and θ_{PLA} are the contact angles of water on fluorocarbon and PLA, respectively, and ϕ_{FC} is the fractional surface coverage of fluorocarbon. Using the literature value for the contact of water on PTFE for θ_{FC} indicates approximate values

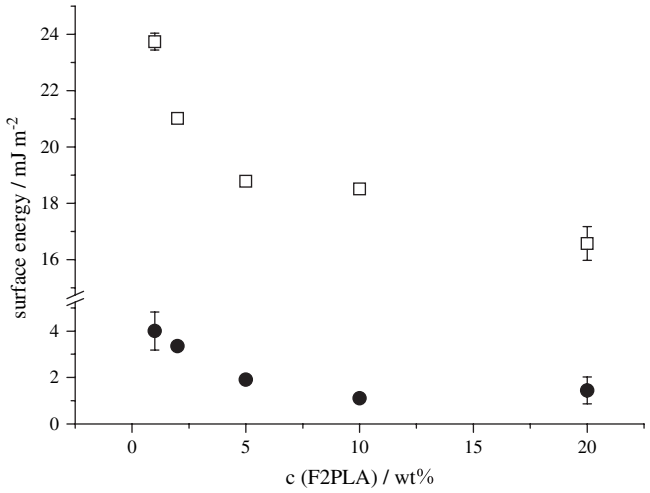

Fig. 5. Derived values of polar (solid circles) and dispersive (open squares) contributions to the blend surface.

for the surface coverage of fluorocarbon of ~80% at F2PLA concentrations of 5% and above.

The RBS data provide a more direct measure of the amount of fluorocarbon at the surface relative to the bulk concentration. Since every F2PLA chain has two C_8F_{17} groups, and there is no other source of fluorine in the film, it is trivial to convert the apparent thickness of C_8F_{17} surface layer in the SIMNRA simulation to a surface concentration of adsorbed chains per unit area. The plateau value for the surface concentration is approximately 1 adsorbed chain for every 3 nm^2 of film surface. The effective area per C_8F_{17} group estimated from the product of the all-*trans* length and the square root of the cross-sectional area of a fluorocarbon chain is approximately 0.7 nm^2. This calculation indicates that approximately 50% of the PLA surface is covered with fluorocarbon at saturation. Although somewhat less than the value derived from the contact angle analysis, this result also confirms that a substantial proportion of the PLA surface is fluorinated by blending with F2PLA, and that the levels of fluorination achieved with this difunctional additive greatly exceed those reported previously for comparable mono-end-functionalized polymers [10,22,26]. The discrepancy between values derived by RBS and contact angle analysis could result from variations in the roughness of the polymer films, orientation of the fluorocarbon groups, or from the assumption that the surface energy of the blend may be represented by a linear combination of the surface energy of the pure components. The RBS data provide a much more direct measure of surface concentration, therefore we should conclude that the saturated surface coverage of fluorocarbon is approximately 50%.

Since ion beam analysis techniques provide a fairly direct measure of concentration versus depth, they are particularly useful for the determination of the surface excess concentration. This is the thermodynamically significant measure of adsorption defined as the difference between the surface concentration and the bulk concentration,

$$z^* = \int_0^\infty \phi(x) - \phi_{\text{bulk}}\, \mathrm{d}x \tag{3}$$

where $\phi(x)$ is the concentration of adsorbate as a function of depth, x, and ϕ_{bulk} is the limiting adsorbate concentration far from the surface. In order to make meaningful comparisons between adsorbed polymers of different molecular weights, the surface excess is often normalized with respect to the radius of gyration, R_g ($= b\sqrt{N/6}$ where N is the degree of polymerisation). Small-angle neutron scattering experiments [31] have shown the statistical step length, b, for PLA to be 1.0 nm, which yields a value of approximately 5.0 nm for the radius of gyration of the F2PLA.

Variation of z^*/R_g as a function of blend concentration is shown in Fig. 6. The increase in normalized surface excess is consistent with the increase in contact angles and the decrease in surface energy. Using the self-consistent mean field theory (SCFT) approach of Shull [4,9], it is possible to relate the normalized surface excess to the thermodynamic 'sticking energy', β, of the end-functionalized polymer to the surface [6]

$$\beta = \chi_b - \chi_s + 1.1 \ln\left(\frac{\delta}{R_g}\right) \tag{4}$$

where χ_s and χ_b are the free energies of interaction of the end-functional group with the surface and bulk, respectively. The logarithmic term accounts for the entropic penalty associated with confining the end-functional group in the surface layer of the lattice, where δ is the size of the lattice layer.

The curves in Fig. 6 show how the equilibrium surface excess predicted by SCFT increases as a function of increasing sticking energy and increasing concentration. At intermediate concentrations, reasonable agreement was found between theory and experiment for $\beta = 6.0 \pm 0.5\ k_BT$, although the measured surface excess is significantly less than the predicted surface excess at the extreme ends of the concentration range examined. We note that this value for β is significantly larger than previously reported values for singly fluorocarbon

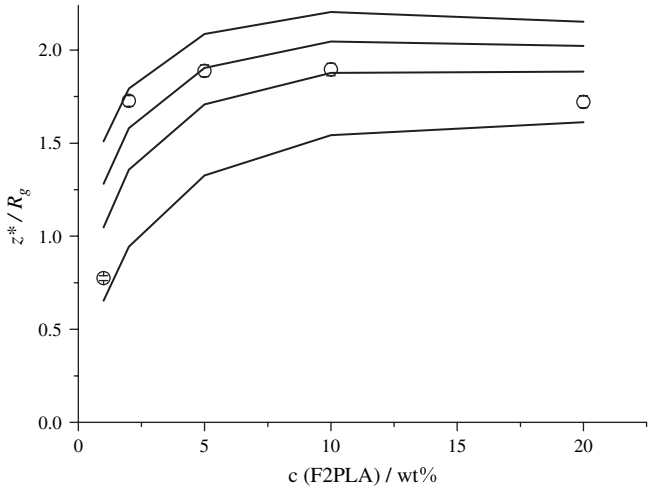

Fig. 6. Normalized surface excess concentration of F2PLA as a function of blend concentration. The solid curves indicate in ascending order, the SCFT predictions for thermodynamic sticking energy per chain end of 4.6, 5.5, 6.0 and 6.5 k_BT.

functionalized polymer chains [10]. This difference reflects the fact that each polymer chain has two large fluorocarbon units, and may also indicate that there is a particularly strong antipathy between fluorocarbons and polylactide that contributes to the surface adsorption. In our calculation of the surface excess, we have deducted the product of the bulk concentration and the radius of gyration from the surface concentration. This correction reduces the surface excess at high concentrations faster than is predicted by the SCFT calculations, possibly indicating that non-adsorbing F2PLA chains are excluded from the surface layer. The most obvious reason for the discrepancy at low concentrations is that the surface excess simply takes longer to develop at lower additive concentrations. Similar behaviour is well established in the case of diffusion limited adsorption [32], wherein the growth of the surface excess is limited by the flux of surface-active additive to the surface.

Although a detailed study of the diffusion of F2PLA additives is beyond the scope of this present paper, we have explored the rate of adsorption F2PLA to film surfaces in which the F2PLA must first diffuse through a layer of PLA. Contact angle and RBS data of bilayer samples confirmed that prior to annealing there was no fluorocarbon at the film surface. After annealing for just 10 min at 90 °C the contact angles with water had increased to 90°, indicating that a significant amount of F2PLA had diffused through the PLA overlayer to the external film surface. On this result alone, we should be confident that in the blended films where F2PLA is already adjacent to the exposed surface, annealing for 1 h at this temperature should be ample to allow equilibration. The true diffusion coefficient of F2PLA was estimated from the rate of growth of the surface excess at short annealing times. The one-dimensional solution to the diffusion equation for a bilayer may be written in terms of the volume fraction of one component,

$$\phi_{\mathrm{F2PLA}}(x,t) = \frac{c}{2}\left[\mathrm{erf}\left(\frac{h+x}{\sqrt{4Dt}}\right) + \mathrm{erf}\left(\frac{h-x}{\sqrt{4Dt}}\right)\right] \quad (5)$$

where c is the initial volume fraction of diffusant (F2PLA) in the substrate layer, h is the thickness of this layer (510 nm), x is the distance from the substrate, D is the diffusion coefficient and t is time. At early stages, F2PLA reaching the polymer surface will adsorb, and diffusion of F2PLA from the surface back into the bulk will be negligible. The growth in surface excess as a function of time can be estimated from numerical integration of Eq. (5) from $x = 955$ nm to infinity with respect to time.

The rate of growth of fluorocarbon concentration at the film surface is shown in Fig. 7. Good agreement between experiment and calculated surface excess at early annealing times was found with $D \sim 160\ \mathrm{nm^2\,s^{-1}}$. At longer annealing times as the surface begins to saturate with F2PLA, the measured rate of adsorption is reduced. Our results clearly demonstrate that F2PLA is able to diffuse throughout the thickness of the films over the 1 h annealing period used in the blended films

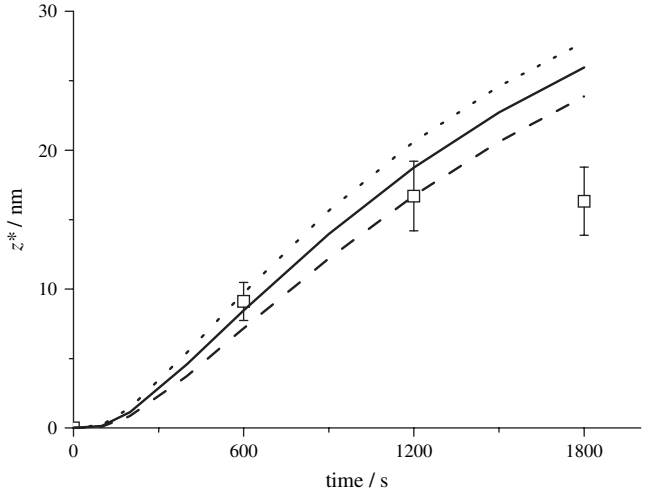

Fig. 7. Rate of development of surface excess in bilayer films as a function of annealing time at 90 °C. The calculated rates of growth for z^* with a diffusion coefficients of 160, 180 and 200 $\mathrm{nm^2\,s^{-1}}$ are given by the dashed, solid and dotted curves, respectively.

therefore the rate of diffusion should not significantly limit the surface excess values measured.

Intriguingly, the apparent surface excess concentrations derived for the annealed bilayer films were slightly larger than for the corresponding blended films. The inconsistency between results for films annealed for 1 h indicates that despite the rapid diffusion, equilibration must be hindered. This result may be understood when one considers the significant polydispersity of the F2PLA additive. The molecular weight range in F2PLA will give rise to a range in the diffusion coefficient of fluorocarbon functionalized chains. By placing a PLA film over the blended film prior to annealing, F2PLA that reaches the film surface will be segregated according to molecular weight such that the small chains arrive first. By analogy to chromatography experiments, the thickness of the upper PLA film will dictate the extent of discrimination between F2PLA chains of differing molecular weight. Since the smallest chains of F2PLA in the distribution contain the largest proportion of fluorocarbon, low molecular weight F2PLA arriving at the film surface will form a stable layer of adsorbate with the relatively high surface fluorocarbon concentration seen. This surface excess layer is likely to restrict the rate at which further F2PLA may adsorb to the surface in the same way as has been established for reactions between end-functionalized polymers and polymer/polymer interfaces [33].

5. Conclusions

We have shown for the first time that a substantial increase in both hydrophobicity and lipophobicity may be imparted to a polymer blend surface using end-functionalized polymers, which are well above their entanglement molecular weight. When annealed above the glass transition temperature, these polymers form a fluorocarbon rich surface layer that approaches the surface characteristics of PTFE even when the bulk polymer contains as little as 0.2% fluorocarbon. Contact

angle data showed significant increases in hydrophobicity and lipophobicity, and analysis of water contact angle data indicates substantial fluorocarbon coverage. There was a dramatic reduction in surface energy with increasing F2PLA content towards limiting values of 17 and 2 mJ m^{-2} for the dispersive and polar components of the blend surface energy, respectively. Surface excess data obtained by Rutherford backscattering measurements show that the surface excess of F2PLA grows to a plateau value of approximately 1 adsorbed chain per 3 nm^2 of blend surface. At this surface concentration we estimate that approximately 50% of the polylactide surface is covered by fluorocarbon. Self-consistent field theory analysis reveals that the thermodynamic sticking energy per adsorbed F2PLA chain is approximately 6 k_BT. Results at low concentrations suggested that surface adsorption might not have reached equilibrium. By analysing the increase in hydrophobicity and surface fluorocarbon concentration of bilayer films in which the F2PLA was initially buried under a 445 nm thick PLA layer showed that adsorption occurred well-within the annealing times used. Analysis of the growth of surface excess in bilayer films yielded a diffusion coefficient of approximately 160 $nm^2 s^{-1}$, although it is likely that this value is dominated by the faster moving smaller F2PLA chains within the molecular weight distribution of the material.

Acknowledgment

We thank Dr. John Clint (University of Hull, UK) for helpful discussions about the contact angle analysis, and Prof. Ken Shull (Northwestern University, USA) for provision of the SCFT fitting code. We are grateful to the EU-RDF and One-NorthEast for funding via the University Innovation Centre in Nanotechnology.

References

[1] Ward LJ, Badyal JPS, Goodwin AJ, Merlin PJ. Polymer 2005;46(12):3986–91.
[2] Garbassi F, Morra M, Occhiello E. Polymer surfaces. From physics to technology. New York: John Wiley and Sons Ltd; 1994.
[3] Mark HF, Bikales NM, Overberger CG, Menges G. In: Kroschwitz JI, editor. Encyclopedia of polymer science and engineering, vol. 3. New York: John Wiley and Sons; 1985.
[4] Shull KR. J Chem Phys 1991;94(8):5723–37.
[5] Auvray L, Auroy P, Cruz M. Journal de Physique I 1992;2(6):943–54.
[6] Jones RAL, Norton LJ, Shull KR, Kramer EJ, Felcher GP, Karim A, et al. Macromolecules 1992;25(9):2359–68.
[7] Clarke CJ, Jones RAL, Edwards JL, Shull KR, Penfold J. Macromolecules 1995;28(6):2042–9.
[8] Mansfield TL, Iyengar DR, Beaucage G, McCarthy TJ, Stein RS, Composto RJ. Macromolecules 1995;28(2):492–9.
[9] Shull KR. Macromolecules 1996;29(7):2659–66.
[10] Hopkinson I, Kiff FT, Richards RW, Bucknall DG, Clough AS. Polymer 1997;38(1):87–98.
[11] O'Rourke-Muisener PAV, Koberstein JT, Kumar S. Macromolecules 2003;36(3):771–81.
[12] O'Rourke-Muisener PAV, Jalbert CA, Yuan CG, Baetzold J, Mason R, Wong D, et al. Macromolecules 2003;36(8):2956–66.
[13] Kiff FT, Richards RW, Thompson RL. Langmuir 2004;20(11):4465–70.
[14] Koberstein JT. J Polym Sci Part B Polym Phys 2004;42(16):2942–56.
[15] Narrainen AP, Hutchings LR, Ansari IA, Clarke N, Thompson RL. Soft Matter 2006;2:126–8.
[16] Li H, Zhang YM, Zhang H, Xue MZ, Liu YG. J Polym Sci Part A Polym Chem 2006;44(12):3853–8.
[17] Bucknall DG, Higgins JS, Rostami S. Polymer 1992;33(20):4419–22.
[18] Hu WC, Koberstein JT, Lingelser JP, Gallot Y. Macromolecules 1995;28(15):5209–14.
[19] Cho BK, Jain A, Gruner SM, Wiesner U. Science 2004;305(5690):1598–601.
[20] Cho BK, Jain A, Nieberle J, Mahajan S, Wiesner U, Gruner SM, et al. Macromolecules 2004;37(11):4227–34.
[21] Osawa S, Yabe M, Miyamura M, Mizuno K. Polymer 2006;47(11):3711–4.
[22] Schaub TF, Kellogg GJ, Mayes AM, Kulasekere R, Ankner JF, Kaiser H. Macromolecules 1996;29(11):3982–90.
[23] Composto RJ, Walters RM, Genzer J. Mater Sci Eng R 2002;38(3–4):107–80.
[24] Tesmer JR, Nastasi M, Barbour JC, Maggiore CJ, Mayer JW. Handbook of modern ion beam materials analysis. Pittsburgh: Materials Research Society; 1995.
[25] Mayer M. SIMNRA user's guide. Garching: Max-Planck-Institut für Plasmaphysik; 1997.
[26] Hutchings LR, Richards RW, Thompson RL, Bucknall DG, Clough AS. Eur Phys J E 2001;5(4):451–64.
[27] Dorgan JR, Janzen J, Knauss DM, Hait SB, Limoges BR, Hutchinson MH. J Polym Sci Part B Polym Phys 2005;43(21):3100–11.
[28] Clint JH, Wicks AC. Int J Adhes Adhes 2001;21(4):267–73.
[29] Owens DK, Wendt RC. J Appl Polym Sci 1969;13(8):1741.
[30] Timmermans J. Physico-chemical constants of pure organic compounds. Amsterdam: Elsevier; 1965.
[31] Anderson KS, Hillmyer MA. Macromolecules 2004;37(5):1857–62.
[32] Zhao X, Zhao W, Sokolov J, Rafailovich MH, Schwarz SA, Wilkens BJ, et al. Macromolecules 1991;24(22):5991–6.
[33] O'Shaughnessy B, Vavylonis D. Eur Phys Lett 1999;45(5):638–44.